

Subnatural linewidth in a strongly-driven closed $F \rightarrow F'$ transition

Sapam Ranjita Chanu, Alok K. Singh, Boris Brun, Kanhaiya Pandey, and Vasant Natarajan*
Department of Physics, Indian Institute of Science, Bangalore 560 012, INDIA

We observe linewidths below the natural linewidth for a probe laser on a *two-level system*, when the same transition is driven by a strong control laser. We take advantage of the fact that each level is made of multiple magnetic sublevels, and use the phenomenon of electromagnetically induced transparency or absorption in multilevel systems. Optical pumping by the control laser redistributes the population so that only a few sublevels contribute to the probe absorption. We observe more than a factor of 3 reduction in linewidth in the D_2 line of Rb in room-temperature vapor. The observations can be understood from a density-matrix analysis of the sublevel structure.

PACS numbers: 42.50.Gy,32.80.Qk,32.80.Xx

The natural linewidth of a two-level transition appears as a fundamental limit to the accuracy with which the transition can be used, either for frequency measurement or as a frequency reference for locking a laser. The natural linewidth is determined by the (inverse of the) lifetime of the excited level. In three-level and other multilevel systems, it is now well known that a strong control laser on an auxiliary transition can be used to modify the lifetime of the excited level; hence the linewidth of the transition being probed by a weak laser can become *subnatural*. The effect, called electromagnetically induced transparency (EIT) or absorption (EIA) [1, 2], arises due to the AC-Stark shift of the levels caused by the control laser (creation of *dressed states* [3]), and subsequent quantum interference of the absorption pathways to these dressed states [4]. The subnatural linewidth observed in these multilevel systems [5, 6] leads to applications in high-resolution spectroscopy [7] and sub-Doppler laser cooling [8], while the anomalous dispersion near the resonance has applications in slowing of light [9] and quantum information processing.

In this work, we show that such subnatural linewidth can also be observed in a *two-level system*, i.e., a system where both the control laser and the probe laser drive the same transition. Of course, this is a two-level system only in the sense that there is no additional level involved and that the lifetime of the upper level limits the linewidth of the transition. We take advantage of the fact that each level is made of multiple magnetic sublevels. Optical pumping by the control laser then causes the population to redistribute among the sublevels, and only a few sublevels contribute to probe absorption. The coherences induced by the control laser cause a subnatural resonance at line center. Our experiments are done in the $5S_{1/2} \rightarrow 5P_{3/2}$ D_2 line of Rb, where we observe more than a factor of three reduction below the natural linewidth. Interestingly, we observe these narrow resonances with room temperature vapor, where the Doppler width is typically $100\times$ larger than the natural linewidth.

The ground state of Rb (and other alkali atoms) consists of two hyperfine levels, thus there are two sets of transitions starting from this state. Though the subnatural feature shows up for both sets of transitions, it appears as enhanced absorption (EIA) in one case and enhanced transmission (EIT) in the other. This is because the dominant transition for the lower-level set is the closed $F \rightarrow F - 1$ transition (with a smaller number of magnetic sublevels in the excited state), while it is $F \rightarrow F + 1$ for the upper-level set (with a larger number of magnetic sublevels in the excited state). The differences between these two sets and the observed line shapes can be understood from a density-matrix analysis of the system.

The subnatural features we observe in our work are also to be contrasted with the phenomenon of coherent-population trapping (CPT) in three-level Λ systems [10, 11], where the linewidth can be extremely narrow compared to the linewidth of the excited state because it is limited only by the decoherence rate between the two ground levels. This phenomenon relies on the use of *phase-coherent* control and probe lasers to drive the atoms into a dark non-absorbing state. The two lasers have to have roughly equal intensities as both are required to drive the atoms into the dark state. Since CPT is a ground-state coherence phenomenon, it is used, for example, for precision spectroscopy of the ground hyperfine interval in atomic clocks [12]. These experiments benefit by the use of vapor cells filled with buffer gas or with paraffin coating on the walls, which increase the ground-coherence time but also shift or broaden the optical transition. Moreover, the relevant natural linewidth in these cases is the inverse of the lifetime of the upper ground level, which can be quite long because the transition is electric-dipole forbidden. The scan axis in CPT experiments is the Raman detuning between the two lasers from the two-photon resonance condition, and not the optical frequency of the probe laser. Thus, if the control laser were detuned from its optical resonance, it will not affect the Raman resonance condition for CPT, but it will shift the resonance location for EIT. In summary, our EIT experiments (i) use a weak probe laser; (ii) can be used for precision spectroscopy on the excited

*Electronic address: vasant@physics.iisc.ernet.in;
URL: www.physics.iisc.ernet.in/~vasant

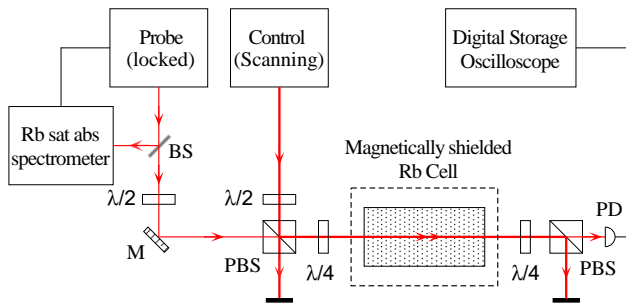


FIG. 1: (Color online) Schematic of the experiment with independent control and probe lasers. For the experiments with phase coherent beams, both beams were derived from the same laser. Figure key: BS – beam splitter, $\lambda/2$ – halfwave retardation plate, $\lambda/4$ – quarterwave retardation plate, M – mirror, PBS – polarizing beamsplitter cube, PD – photodiode.

state [7]; (iii) use pure vapor cells; and (iv) have a scan axis (showing the subnatural feature) that is the optical frequency of the *phase-independent* probe laser.

The experimental set-up is shown schematically in Fig. 1. The control and probe beams are derived from two *independent* home-built diode laser systems operating on the 780 nm D_2 line of ^{87}Rb [13]. The linewidth of the lasers after feedback stabilization is about 1 MHz. The beams are elliptic and have a size of 2 mm \times 3 mm. The probe beam is locked to a hyperfine transition using saturated-absorption spectroscopy (SAS) in a vapor cell. The control beam is scanned around the same transition. The two beams have orthogonal circular polarizations (σ^+ and σ^-) and co-propagate through a vapor cell. The cell has a multilayer magnetic shield that reduces the stray fields to below 1 mG. The two laser beams are mixed and separated using polarizing beam splitter cubes (PBS), and the probe beam is detected with a photodiode. The individual beam powers are controlled using halfwave retardation plates before the PBS's. We have shown earlier [14] that the use of co-propagating beams eliminates crossover resonances, and that by scanning the control laser while keeping the probe fixed makes the signal appear on a Doppler-free background.

The first set of experiments was done for transitions starting from the upper ground level in ^{87}Rb , i.e., on the closed $F = 2 \rightarrow F' = 3$ transition. The results for a probe power of 8 μW and control power of 150 μW are shown in Fig. 2. The spectrum shows a broad (≈ 20 MHz wide) transparency peak as the control is scanned. This is the usual resonance occurring due to EIT and saturation effects seen in pump-probe spectroscopy [14]. Exactly at line center, a narrow EIA dip (corresponding to enhanced absorption) appears. The full-width-at-half-maximum (FWHM) of the narrow resonance is only 1.8 MHz compared to the natural linewidth of 6 MHz. The subnatural feature is robust and the FWHM remains less than 3 MHz (0.5Γ) with increase in control power to 250 μW . But as the control power is increased, the depth of the resonance and its signal-to-noise ratio increases. For

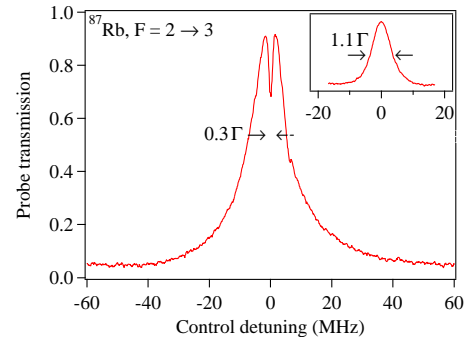


FIG. 2: (Color online) Subnatural EIA resonance for upper-level transitions obtained with the probe laser locked to the $F = 2 \rightarrow F' = 3$ transition and control laser scanning across the same transition. The inset shows a typical SAS spectrum, which has a linewidth of 1.1Γ .

comparison, a typical SAS spectrum (taken with counter-propagating beams) is shown in the figure inset. With optimal powers in the pump and probe beams, the linewidth is 6.6 MHz (1.1Γ).

To understand this theoretically, we consider the magnetic sublevel structure shown in Fig. 3. For the $2 \rightarrow 3$ transition, there are 5 and 7 sublevels respectively. Optical pumping by the circularly-polarized control will transfer all the population into the $m_F = +2$ ground sublevel, as shown in Fig. 3(a). If we therefore ignore the other sublevels, we have a V-type system formed by the $m_{F'} = +1 \leftrightarrow m_F = +2 \leftrightarrow m_{F'} = +3$ sublevels. Dressing of the $m_F = +2$ and $m_{F'} = +3$ sublevels by the strong control laser will cause the usual transparency resonance (EIT) for the weak probe laser. Now consider that the control is also going to dress the $m_F = 0$ and $m_{F'} = +1$ sublevels, forming effectively an N -type system [15, 16]. The additional coherences induced by this is what causes the narrow EIA resonance.

We have done a standard density-matrix analysis of this system to confirm the above explanation. The calculation takes into account Doppler averaging in room-temperature vapor. In Fig. 3(b), we show the calculated spectrum considering the N -type system formed by the $m_F = 0$ and $+2$ sublevels. The Rabi frequency of the control laser is taken to be 6 MHz, which corresponds to the experimental power if we assume that the entire power is spread uniformly over the beam size. To account for the finite linewidth of the control laser, we assume that the ground sublevels decohere at a rate of 1 MHz. There are no other adjustable parameters. The calculated spectrum reproduces the features of the observed spectrum shown in Fig. 2, with a broad EIT peak and a narrow EIA dip at line center. We have verified that the EIA dip disappears if we do not consider the dressing of the $m_{F'} = +1$ sublevel. Furthermore, the depth of the EIA resonance increases with increasing Rabi frequency of the control, exactly as observed experimentally. The calculation also shows that the width of the EIA dip be-

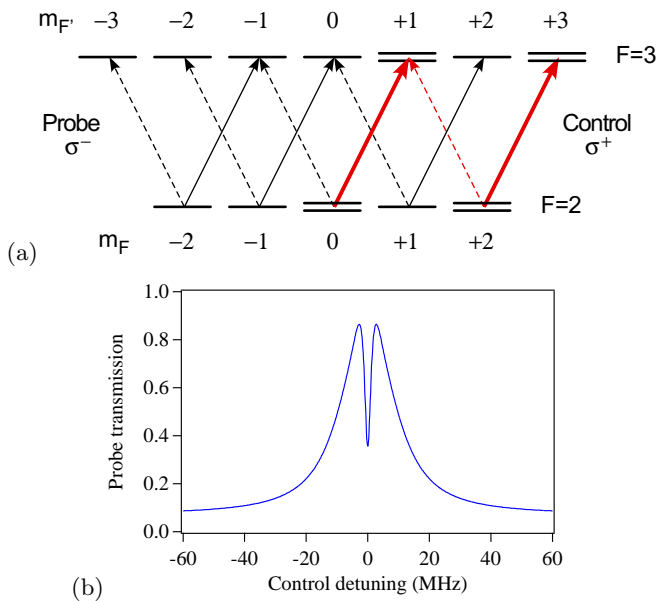


FIG. 3: (Color online) Theoretical study of upper-level transitions. (a) Sublevel structure for the $F = 2 \rightarrow F' = 3$ transition. Optical pumping causes only the $m_F = 0$ and $m_F = +2$ sublevels to contribute. (b) Calculated spectrum for the N -type system in (a).

comes smaller at smaller control powers, but observing linewidths below 1.5 MHz is experimentally challenging because the probe laser itself has a linewidth of 1 MHz.

The next set of experiments was done for transitions starting from the lower ground level in ^{87}Rb , i.e., with the lasers on the closed $F = 1 \rightarrow F' = 0$ transition. The spectrum obtained with a probe power of $8 \mu\text{W}$ and a smaller (compared to the previous set) control power of $80 \mu\text{W}$ is shown in Fig. 4(a). In this case, the measured spectrum has a central *transparency* peak surrounded by broad enhanced absorption wings. The EIT peak at line center is *subnatural*, with a linewidth of only 2.4 MHz (0.4Γ). For comparison, we again show in the inset a typical SAS spectrum taken with optimal pump and probe powers. The linewidth of 12 MHz is 5 times larger than the one for the “controlled” case.

As before, the features of the measured spectrum can be understood theoretically. In this case, the sublevel structure is quite simple, with 3 sublevels in the lower level and 1 sublevel in the upper level. The circularly-polarized beams couple these sublevels to form a Λ -type system, as shown in the inset of Fig. 4(b). The calculated spectrum, using a Rabi frequency of 4.4 MHz (because the control power is a factor of 2 smaller) and taking into account thermal averaging, reproduces the features of the observed spectrum including the enhanced-absorption wings. This can be understood as follows. Off resonance, the strong control laser optically pumps the population into the $m_F = +1$ sublevel, which causes increased probe absorption. As the control comes into resonance, there are additional induced coherences, which

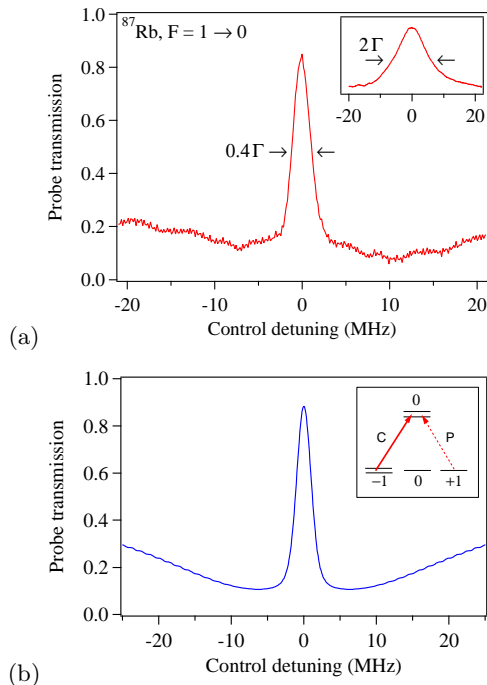


FIG. 4: (Color online) Subnatural EIT resonance for lower-level transitions. (a) Measured spectrum with the probe laser locked to the $F = 1 \rightarrow F' = 0$ transition. The inset shows a typical SAS spectrum for the same transition. (b) Calculated spectrum for the Λ -type system shown in the inset.

causes the EIT resonance. It is well known that in Λ systems the EIT resonance can be subnatural [4, 5]. The calculated spectrum has a width similar to the measured one.

As in the case of upper-level transitions, the FWHM of the central resonance remains below 3 MHz even with a control power of $250 \mu\text{W}$, while its signal-to-noise ratio increases. We are also able to go to lower control powers of about $40 \mu\text{W}$ and still see a prominent resonance. But the linewidth does not decrease much, probably again because of the 1-MHz linewidth of the probe laser.

In the above experiments, we have considered the closed transition in each set, partly because it is a better realization of a two-level system, and partly because we can do a more rigorous theoretical calculation without worrying about the presence of the other levels. This is not the case for open transitions because we have to consider the effect of optical pumping into the closed transition. However, experimentally we find the same behavior for the open transitions also. The results for the $2 \rightarrow 2$ and $1 \rightarrow 1$ transitions are shown in Fig. 5. The control powers are $150 \mu\text{W}$ and $40 \mu\text{W}$, respectively. As before, we see enhanced absorption for the upper-level transition [shown in (a)] and enhanced transmission for the lower-level transition [shown in (b)]. The line shapes and widths are similar to the closed transitions, because the closed transition is the dominant transition in each set and takes over after a few absorption-emission cycles.

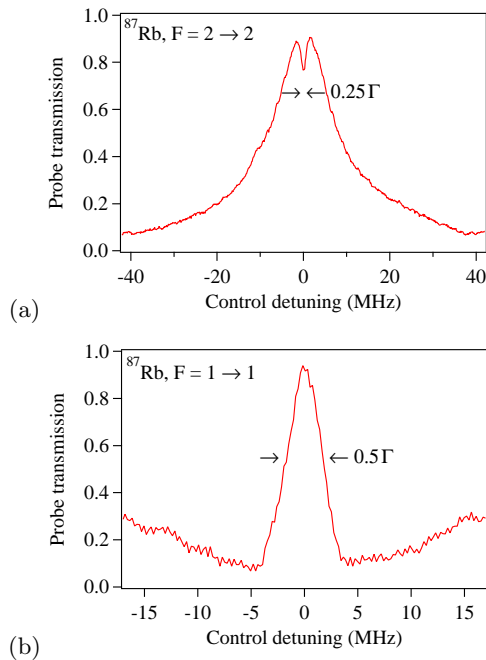


FIG. 5: (Color online) Subnatural resonances for the open transitions. (a) is for upper-level transitions showing enhanced absorption, while (b) is for lower-level transitions showing enhanced transparency. The widths are similar to what is observed for the closed transitions.

We thus see that the subnatural feature is quite robust, appearing for both closed and open transitions, and for control powers ranging from 5 to 30 times the probe power. It appears even with linear polarization of the two beams and does not seem to require circular polarization. In addition, it appears without the magnetic shield around the cell so that the sublevels are not degenerate. Finally, since our cell contains both isotopes of Rb, we can do the same experiments with the other isotope, namely ^{85}Rb . We observe the same behav-

ior, i.e., an enhanced-absorption subnatural resonance for upper-level transitions ($F = 3 \rightarrow F'$) and an enhanced-transmission subnatural resonance for lower-level transitions ($F = 2 \rightarrow F'$).

In conclusion, we have observed linewidth reduction below the natural linewidth in a two-level system when a strong control laser is applied to the same transition. We take advantage of the presence of multiple magnetic sublevels in each level and the phenomenon of electromagnetically induced transparency or absorption, a phenomenon that is well studied in multilevel systems. In this effect, the control laser causes population redistribution and “dressing” of the sublevels, and the linewidth reduction comes about because of interference among the absorption pathways. We observe these subnatural resonances in the D_2 line of ^{87}Rb using room-temperature atoms in a vapor cell. There are two sets of hyperfine transitions starting from the two ground hyperfine levels, and we observe the subnatural feature for both sets. However, it appears as an enhanced-absorption dip for upper-level transitions, and as an enhanced-transparency peak for lower-level transitions. This difference can be understood from the differences in the number of magnetic sublevels for the dominant closed transition in each set. The observed line shapes and widths are reproduced by density-matrix calculations. We observe more than a factor of 3 reduction in linewidth below the natural linewidth, while conventional saturated-absorption spectroscopy gives linewidths that are 1 to 2 times the natural linewidth. These subnatural features and the consequent anomalous dispersion should prove useful in high-resolution spectroscopy and other applications of EIT since they appear exactly at line center.

This work was supported by the Department of Science and Technology, India. V.N. acknowledges support from the Homi Bhabha Fellowship Council; and A.K.S. and K.P. from the Council of Scientific and Industrial Research, India.

-
- [1] S. P. Tewari and G. S. Agarwal, *Phys. Rev. Lett.* **56**, 1811 (1986).
 [2] K.-J. Boller, A. Imamoglu, and S. E. Harris, *Phys. Rev. Lett.* **66**, 2593 (1991).
 [3] C. Cohen-Tannoudji and S. Reynaud, *J. Phys. B.* **10**, 365 (1977).
 [4] Y.-q. Li and M. Xiao, *Phys. Rev. A* **51**, 4959 (1995).
 [5] U. D. Rapol, A. Wasan, and V. Natarajan, *Phys. Rev. A* **67**, 053802 (2003).
 [6] S. M. Iftiqar, G. R. Karve, and V. Natarajan, *Phys. Rev. A* **77**, 063807 (pages 5) (2008), URL <http://link.aps.org/abstract/PRA/v77/e063807>.
 [7] U. D. Rapol and V. Natarajan, *Europhys. Lett.* **60**, 195 (2002).
 [8] G. Morigi and E. Arimondo, *Phys. Rev. A* **75**, 051404 (pages 4) (2007), URL <http://link.aps.org/abstract/PRA/v75/e051404>.
 [9] L. V. Hau, S. E. Harris, Z. Dutton, and C. H. Behroozi, *Nature (London)* **397**, 594 (1999).
 [10] G. Alzetta, A. Gozzini, L. Moi, and G. Orriols, *Il Nuovo Cimento B* **36**, 5 (1976).
 [11] E. Arimondo, *Progress in Optics*, vol. 35 (Elsevier Science, Amsterdam, 1996).
 [12] R. Wynands and A. Nagel, *Appl. Phys. B* **68**, 1 (1999).
 [13] A. Banerjee, U. D. Rapol, A. Wasan, and V. Natarajan, *Appl. Phys. Lett.* **79**, 2139 (2001).
 [14] A. Banerjee and V. Natarajan, *Opt. Lett.* **28**, 1912 (2003).
 [15] C. Goren, A. D. Wilson-Gordon, M. Rosenbluh, and H. Friedmann, *Phys. Rev. A* **69**, 053818 (2004).
 [16] M. G. Bason, A. K. Mohapatra, K. J. Weatherill, and C. S. Adams, *Journal of Physics B: Atomic, Molecular and Optical Physics* **42**, 075503 (2009), URL <http://stacks.iop.org/0953-4075/42/i=7/a=075503>.